Endohedrally Functionalized Metal–Organic Cage-Crosslinked Polymer Gels as Modular Heterogeneous Catalysts

Christopher M. Brown,[a]† David J. Lundberg,[a,b]† Jessica R. Lamb,[a] Ilia Kevlishvili,[b] Denise Kleinschmidt,[a] Yasmeen S. Alfaraj,[a] Heather J. Kulik,[b] Maria Francesca Ottaviani,[c] Nathan J. Oldenhuis[a,d]* and Jeremiah A. Johnson[a,e]*

[a] Department of Chemistry, Massachusetts Institute of Technology, 77 Massachusetts Avenue, Cambridge, MA 02139, USA

[b] Department of Chemical Engineering, Massachusetts Institute of Technology, 77 Massachusetts Avenue, Cambridge, MA 02139, USA

[c] Department of Pure and Applied Sciences, University of Urbino, Urbino 61029, Italy

[d] Present Address: Department of Chemistry, University of New Hampshire, 23 Academic Way, Durham, NH 03824, USA

[e] David H. Koch Institute for Integrative Cancer Research, Massachusetts Institute of Technology, 77 Massachusetts Avenue, Cambridge, Massachusetts 02139, USA

† Equal contribution.

Abstract: The immobilization of homogeneous catalysts onto supports to improve recyclability while maintaining catalytic efficiency is often a trial-and-error process limited by poor control of the local catalyst environment and few strategies to append catalysts to support materials. Here, we introduce a modular heterogenous catalysis platform that addresses these challenges. Our approach leverages the well-defined interiors of self-assembled $Pd_{12}L_{24}$ metal–organic cages/polyhedra (MOCs): simple mixing of a catalyst-ligand ligand of choice with a polymeric ligand, a spacer ligands, and a Pd salt induces self-assembly of acetylene-linked $Pd_{12}L_{24}$-crosslinked polymer gels featuring endohedrally-catalyst-functionalized junctions. Semi-empirical calculations show that catalyst incorporation into these MOC junctions does not affect their geometry, giving rise to well-defined nanoconfined catalyst domains as confirmed experimentally using several techniques. Given the unique network topology of these freestanding gels, they are mechanically robust regardless of their endohedral catalyst composition, allowing them to be physically manipulated and transferred from one reaction to another to achieve multiple rounds of catalysis. Moreover, by decoupling the catalyst environment (interior of MOC

junctions) from the physical properties of the support (the elastic polymer matrix), this strategy enables catalysis in environments where homogeneous catalyst analogs are not viable, as demonstrated for the Au(I)-catalyzed cyclization of 4-pentynoic acid in aqueous media.

Introduction: The development of reusable, effective, and selective catalysts is imperative for the implementation of sustainable chemical practices and continues to drive innovation in the chemical sciences.[1,2] Heterogenous catalysts have long been at the forefront of this endeavor due to their recyclability and ease of isolation from reactants and product mixtures.[3,4] Despite these advantages, developing heterogeneous catalysts *de novo* is challenging as mechanistic features of a catalytic process are more difficult to study in the solid state.[5–7] By contrast, homogeneous catalytic processes are often easier to study and optimize on the basis of mechanistic insights but are inherently less amenable to facile catalyst recovery and reuse.[8,9] Ideally, one could transfer well-defined homogeneous catalytic systems directly to solid, freestanding supports with robust mechanical properties in a modular and reliable way without diminishing catalyst activity and/or selectivity.[10–15]

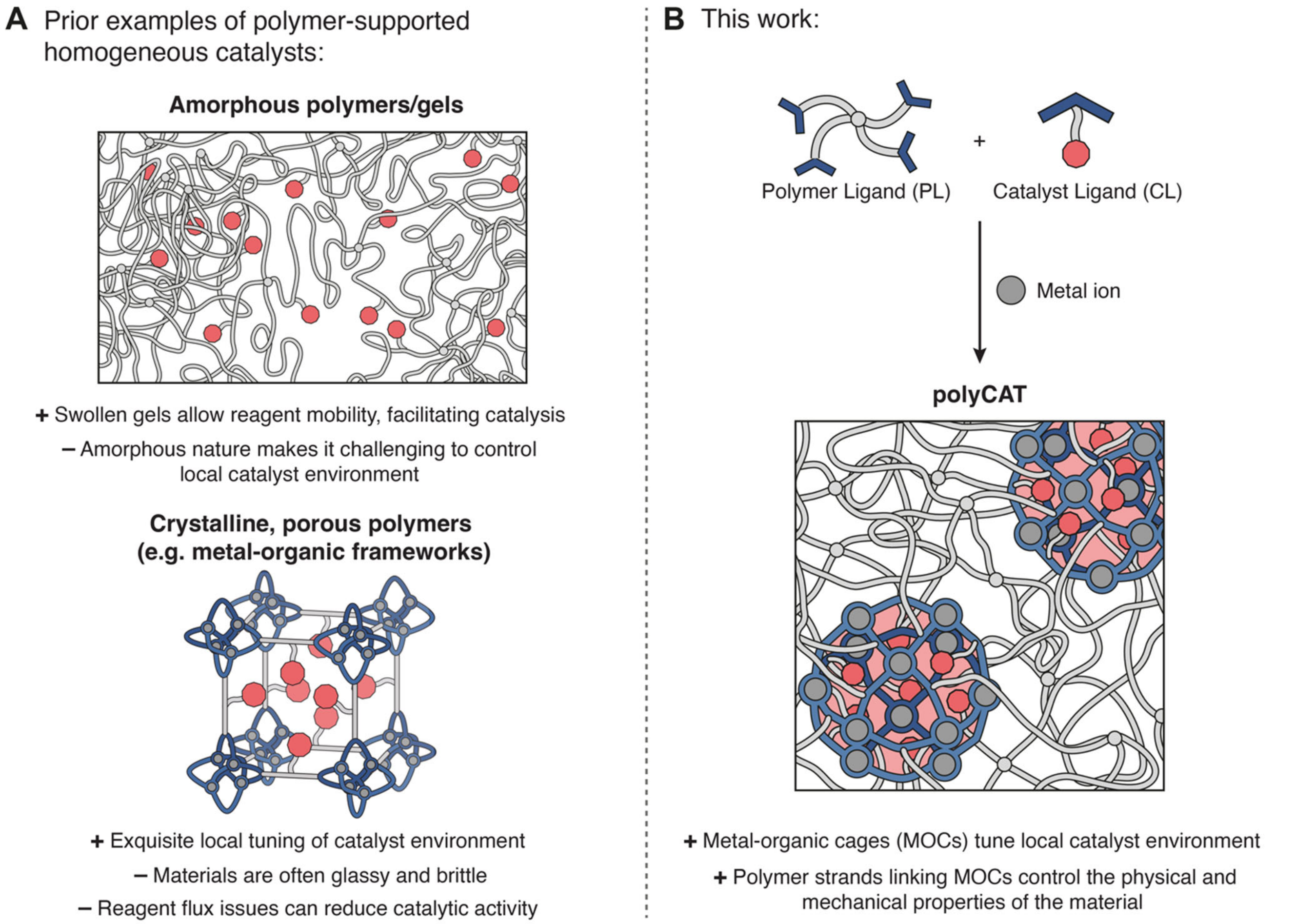

Fig. 1. A, Previous methods to immobilize traditionally homogeneous catalysts have involved the use of polymer networks, or metal-organic frameworks (MOFs). However, these approaches typical result in a trade-off between catalytic activity, and desirable materials properties. **B**, The polyMOC catalyst-containing network (polyCAT) uses the templated assembly of metal organic cages (MOCs) to allow tunable and predictable catalyst environments regardless of catalyst identity. The polymer strands linking the MOCs dictate the physical and mechanical properties of the material, and can be changed without altering the catalyst environment.

Toward this end, the immobilization of homogenous catalysts onto amorphous crosslinked or self-assembled (co)polymers is a common strategy that benefits from the compositional diversity, synthetic flexibility, and tunable physical properties of polymers (Fig. 1a).[12,16–18] When such catalyst-functionalized polymer networks are in a highly swollen gel state, reagent mobility can approach that within solution, facilitating reasonable reaction rates.[19–26] Moreover, the mechanical robustness of synthetic polymers can allow for repeated reuse of such materials and facile physical manipulation. Nevertheless, the amorphous nature of such materials makes it difficult to control the local catalyst environment, giving rise to unpredictable outcomes and potential batch-to-batch variation. Crystalline polymer networks, including coordination polymers such as metal–organic frameworks (MOFs),[27–29] can overcome this challenge by enabling exquisite local tuning of catalyst environments; however, such materials are often brittle powders, lacking mechanical robustness to form into robust freestanding materials.[30] Moreover, these materials often require harsh and extended annealing conditions for their formation, give low catalyst incorporation yields (typically <50%),[29,31–33] and they can suffer reagent flux issues to and from their crystalline pores, leading to catalysis primarily at surface defect sites and lowered catalytic efficiency compared to homogeneous processes.[34–36] For example, in TEMPO-catalyzed oxidation reactions within the pores of a Zr-based MOF, the catalytic efficiency decreased as MOF crystal size increased, suggesting mass transfer limitations to the MOF interior.[32]

An ideal heterogeneous catalysis platform would (1) be easy to form in high yield under mild conditions; (2) enable modular conjugation of structurally distinct homogeneous catalysts to facilitate a range of mechanistically distinct catalytic transformations; (3) provide a precisely defined, tunable, and predictable local catalyst environment that is distinct from the support; (4) possess good mechanical properties to facilitate physical manipulation; (5) allow for changing of the support composition to facilitate use in different solvents/conditions; and (6) would maintain, or even improve, catalyst function compared to the analogous homogeneous reaction conditions. Here, we develop proof-of-concept of such a system by leveraging the unique topological features of metal–organic cage/polyhedra (MOC)-crosslinked polymer gels,[37–47] where $Pd_{12}L_{24}$ MOCs serve as nanoscale junctions that provide discrete local catalyst environments analogous to the unit cell of a MOF, and polymer strands that link MOCs control the physical and mechanical properties of the materials, offering the robust mechanical properties of polymers (Fig. 1b).[42–47] In other words, this strategy combines mechanical property advantages of traditional polymers with the modularity and precision of MOFs. Our materials, which we refer to herein as "polyCATs," form within hours under mild heating from simple mixing of 3–4 components, depending on the need: (i) endohedral catalyst-functionalized ligands (CLs), (ii) exohedral polymer-functionalized ligands (PLs), (iii) spacer ligands (SLs) where necessary to accommodate larger catalysts, and (iv) metal ions (e.g., Pd(II)). Using a combination of shear rheology, electron paramagnetic resonance (EPR) spectroscopy, small-angle X-ray scattering, and semi-empirical calculations, we demonstrate that polyCATs are mechanically robust materials with hierarchical structures that are not perturbed upon catalyst incorporation compared to $Pd_{12}L_{24}$ metal–organic cage (polyMOC) gels lacking endohedral catalysts.[42,44,45] I.e., catalyst incorporation within MOC junctions does not disrupt the overall network structure/topology. Moreover, the fast transport of substrates into the bulk of these gels leads to similar catalytic efficiency compared to homogeneous catalysts, as demonstrated using two mechanistically distinct catalytic transformations (a TEMPO-catalyzed oxidation and a Au(I)-mediated cyclization) that have previously been studied under homogeneous conditions and in the context of MOFs.[48] Here, the mechanical robustness and freestanding nature of polyCATs allows for simple transfer of the material from one reaction to the next with tweezers, allowing for multiple rounds of catalysis without filtration steps. Additionally, the solution phase assembly of polyCATs proceeds in a matter of hours with high yields and incorporation of catalyst moieties (>95%), further demonstrating the utility of this platform when compared to other materials. For instance, TEMPO-appended dicarboxylate ligands have been used in the fabrication of UiO-type MOFs as noted above, but >24 h were required for fabrication, giving ~10–50% yields of catalytic particles with sub-stoichiometric catalyst incorporation.[32,49,50] Finally, by leveraging the water-swellability of a polyCAT featuring polyethylene glycol (PEG)-based strands, we demonstrate the cyclization of 4-pentynoic acid to the corresponding lactone under aqueous conditions where the catalysts themselves are inactive due to poor solubility. This reaction could be repeated twelve times with the same polyCAT material without loss of activity. Altogether, polyCATs could offer a new platform to rapidly translate homogeneous catalysts into heterogeneous variants using freestanding, mechanically robust polymer networks, exploiting the best features of polymers and MOCs.

Results and Discussion

TEMPO-polyCAT design, synthesis, and application to alcohol oxidation reactions. To test the viability of the polyCAT concept, we first targeted a TEMPO-catalyzed oxidation reaction[51] that had previously been reported to proceed under homogeneous conditions and within the pores of mesoporous silica using $Pd_{12}L_{24}$ MOCs.[52,53] Here, the same TEMPO-conjugated bis-*para*-pyridine ligand **TEMPO-CL**[52] was used along with a novel four-arm polyethylene glycol (PEG) star polymer terminated with bis-*para*-pyridine ligands **PEG-PL** (Fig. 2a, see Supporting Information section "Materials and Methods" for gel formation conditions). We define the "C:P" ratio as the average number of bis-pyridyl units in each $Pd_{12}L_{24}$ cage that derive from the catalyst ligand (e.g., **TEMPO-CL**) and the polymer ligand (e.g., **PEG-PL**), respectively. Three C:P ratios were screened—9:1, 7:1, and 5:1—to balance a high catalyst loading (higher C:P) with minimal catalyst leaching into solution (lower C:P); as C:P increases, there is increased likelihood for formation of TEMPO-containing MOCs that are not bound to polymer strands (see Supporting Information section "Statistical Analysis of Catalyst Ligand Distribution within MOCs" for a discussion of the statistics of MOC formation using a binary ligand mixture). Each mixture was combined with $[Pd(MeCN)_4][BF_4]_2$ in DMSO (65 mM Pd(II) in a 5 wt/wt % **PEG-PL** solution) and annealed for 4 h at 60 °C. The resulting gels were soaked 4 times for 4 h each in excess $CDCl_3$ and the supernatants of each wash were collected and analyzed via quantitative electron paramagnetic resonance (EPR) spectroscopy (Figs. S1–2, see Supporting Information section "EPR Studies" for details). In each case, the catalyst incorporation was quite high, with only 5.3%, 4.5% and 2.6% of the **TEMPO-CL** not incorporated into the materials prepared from 9:1, 7:1 and 5:1 C:P ratios, respectively (Table S1). We note that these gels represent the first materials, to our knowledge, to be crosslinked with acetylene-linked, ~4.6 nm diameter $Pd_{12}L_{24}$ MOCs.[54]

As the lowest amount of catalyst leaching was seen in gels prepared using a 5:1 C:P ratio, we chose to move forward with this system for subsequent studies, referring to the material as "**TEMPO-polyCAT**." In addition to limiting catalyst leaching and simultaneously providing a high average catalyst loading of 20 catalysts per MOC junction, this material features an average of 4 polymer strands per MOC junction, thus matching the branch functionality of the PL and providing for a robust "A_4 + B_4"-like network topology.[45] Cross polarization-magic angle spinning (CP-MAS) ^{1}H NMR spectroscopy (Fig. S3) and small-angle X-ray scattering (SAXS, Fig. S4) were used to characterize the structure of **TEMPO-polyCAT**. The former shows characteristic peak broadening and shifting associated with pyridine–Pd coordination-driven assembly while the latter displayed peaks associated with the average inter-MOC spacing and MOC form factor.[42–46] **TEMPO-polyCAT** is a freestanding elastic material with a storage modulus, G', of 28 kPa at 10 rad/s as determined by linear shear rheology frequency sweep experiments (Fig. 2b). Notably, an analogous gel control gel prepared from **PEG-PL** but using a non-catalyst-functionalized methoxy spacer ligand (**SL**) with the same C:P ratio displayed nearly identical frequency sweep behavior (Fig. 2b), suggesting that catalyst incorporation is decoupled from the overall network mechanics and that the network structures are similar in the presence or absence of TEMPO.

Electron paramagnetic resonance (EPR) spectroscopy was used to gain a deeper understanding of the local nitroxide environment in **TEMPO-polyCAT**. Compared to **TEMPO-CL**, the EPR spectrum of **TEMPO-polyCAT** was significantly broadened as expected for immobilized free radicals (Fig. 2c).[55–57] Fitting the spectra revealed clear signs of reduced nitroxide mobility and strong spin-spin exchange interactions, indicative of the nitroxides being crowded within the MOC junctions (see Supporting Information section "EPR Studies" for details). Moreover, the fitting indicated that 94% of the nitroxides existed within a similar chemical environment, which is expected given the symmetry of the MOC junctions (Table S2). Remarkably, the spectrum for **TEMPO-polyCAT** was nearly identical to that of a soluble MOC composed of 20:4 **TEMPO-CL** and a methoxy-functionalized spacer ligand **SL** (Fig. 2c). In other words, introduction of polymer linkers to the exterior of the MOCs does not significantly perturb the catalyst environment.[52] Additionally, this result provides strong evidence for the existence of well-formed MOC junctions within **TEMPO-polyCAT**, as the EPR spectrum for an unannealed material with ill-defined metal–organic crosslinks clearly showed a larger distribution of distinct nitroxide environments (see Supporting Information section "EPR Studies" for details).

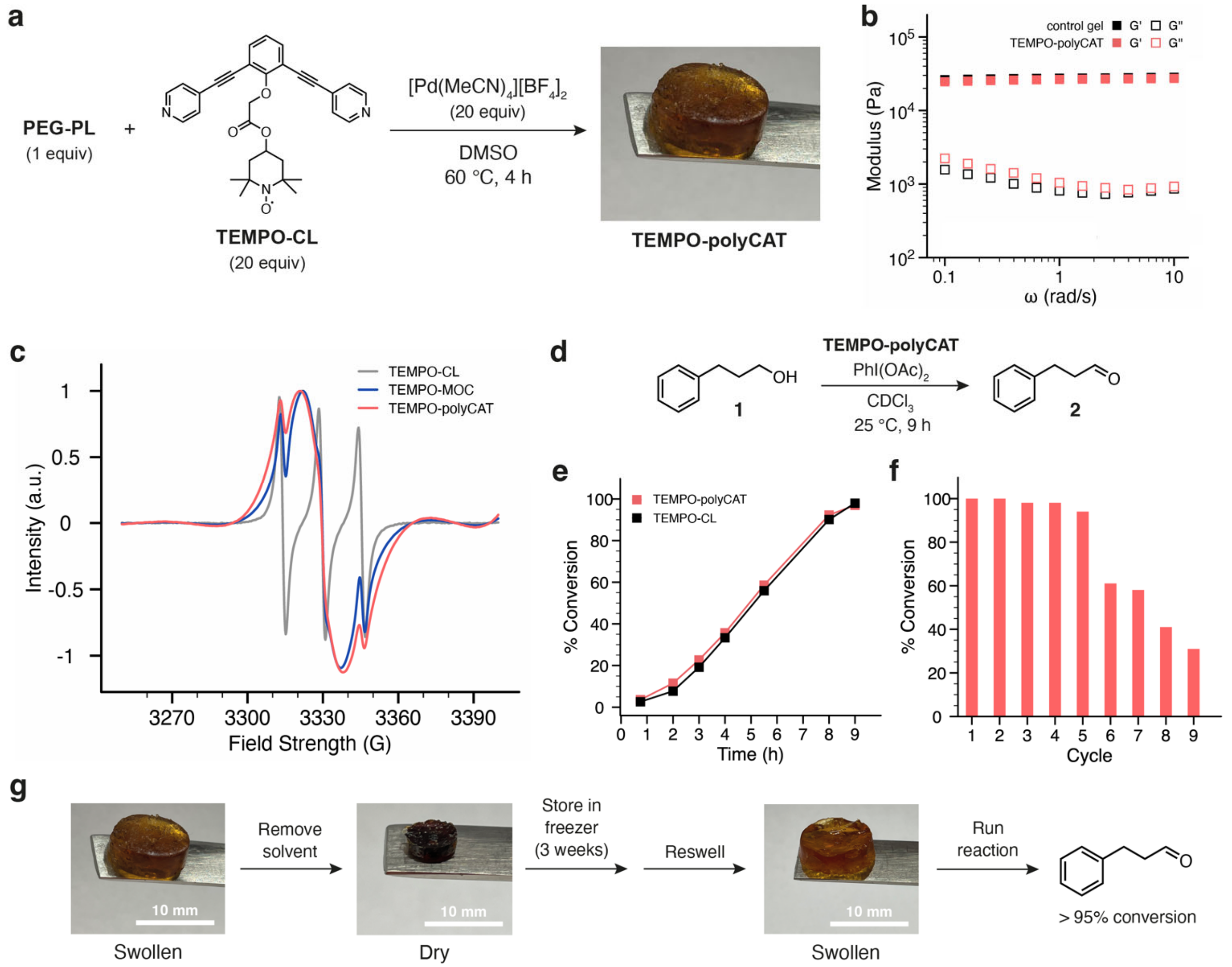

Fig. 2. Analysis of the structure and reactivity of the **TEMPO-polyCAT** gel. **a**, Scheme and image showing the synthesis of the freestanding polyCAT gel. **b**, Comparison of a control gel (black) with an unfunctionalized ligand to the **TEMPO-polyCAT** (red) using a frequency sweep in a sheer rheometer. **c**, EPR spectra showing **TEMPO-CL** ($CHCl_3$), **TEMPO-CL** assembled as MOCs (**TEMPO-MOC**, $CHCl_3$) and **TEMPO-polyCAT**. **TEMPO-polyCAT** shows significantly broadened peaks compared to **TEMPO-CL,** indicative of strong spin-spin interactions resulting from spatially localized TEMPO molecules. **d**, The oxidation of 3-phenyl-1-propanol (**1**) to its corresponding aldehyde (**2**) using **TEMPO-polyCAT**. **e**, Comparison of the rate of oxidation of **TEMPO-CL** free in solution (black) and **TEMPO-polyCAT** gel (red, n=1). **f**, Cycling of the oxidation using **TEMPO-polyCAT**. Conversions are calculated from the integrations of the ^{1}H NMR spectrum of the catalytic solution, using an internal standard (n=1). **g**, Deswelling, storage, and swelling of the material does not diminish the catalytic activity.

To investigate the activity of **TEMPO-polyCAT** as a heterogeneous catalyst for alcohol oxidation, a solution of 3-phenyl-1-propanol (**1**, 1.0 equiv) and diacetoxyiodobenzene (1.2 equiv) in $CDCl_3$ (0.1 M) with tetrakis(trimethylsilyl)silane as an internal standard was added to a 1 mL reaction solution containing a 200 mg TEMPO-polyCAT gel (0.02 mmol **TEMPO-CL**, 10 mol % relative to 3-phenyl-1-propanol) (Fig. 2d). Following a short induction period, >95% conversion of **1** to the corresponding aldehyde **2** was observed within 9 h, with a turnover frequency (TOF) of 1.1 h^{-1} (Fig. 2e). Moreover, the extent of conversion as a function of time was nearly identical to a homogeneous reaction using the same loading of **TEMPO-CL** as the catalyst (Fig. 2e). To ensure catalyst leaching was not responsible for the observed catalytic activity of **TEMPO-polyCAT**, the same reaction was run using the supernatant collected after washing a freshly prepared **TEMPO-polyCAT** sample four times with chloroform; conversion was <3% after 24 h. Additionally, the activity of the supernatant at the end of the catalytic reaction was tested: **TEMPO-polyCAT** was removed from the mixture and an additional portion of **1** and oxidant were introduced to the solution. After 10 h, less than 5% of the new substrate was converted to **2**. These results strongly suggest that the catalytic behavior of **TEMPO-polyCAT** is driven by the endohedrally-bound TEMPO catalysts within the MOC network junctions.

Highlighting the utility of **TEMPO-polyCAT** as a heterogeneous system, the material was cycled through 9 × 12 h rounds of the above reaction with 3 × 30 min washes between each cycle. ^{1}H NMR conversion of **1** to **2** was >95% for the first 5 cycles and decreased during cycles 6–9 (Fig. 2f), meaning that the gel maintains >75% of its original activity for the first 5 cycles. While **TEMPO-polyCAT** maintained its gel form throughout this process, it became grey in color after 9 reaction cycles, perhaps indicating decomposition of TEMPO. Nevertheless, this performance over 9 cycles corresponds to nearly an order-of-magnitude increase in the catalyst turnover number (TON). Finally, to demonstrate the long-term storability of **TEMPO-polyCAT**, a sample was fabricated, dried under a stream of nitrogen for 30 min, and stored at –20 °C for 3 weeks. After this time, the material was swelled in $CDCl_3$ and used to catalyze the oxidation of **1**; no loss in activity was observed (>95% NMR conversion, Fig. 2g).

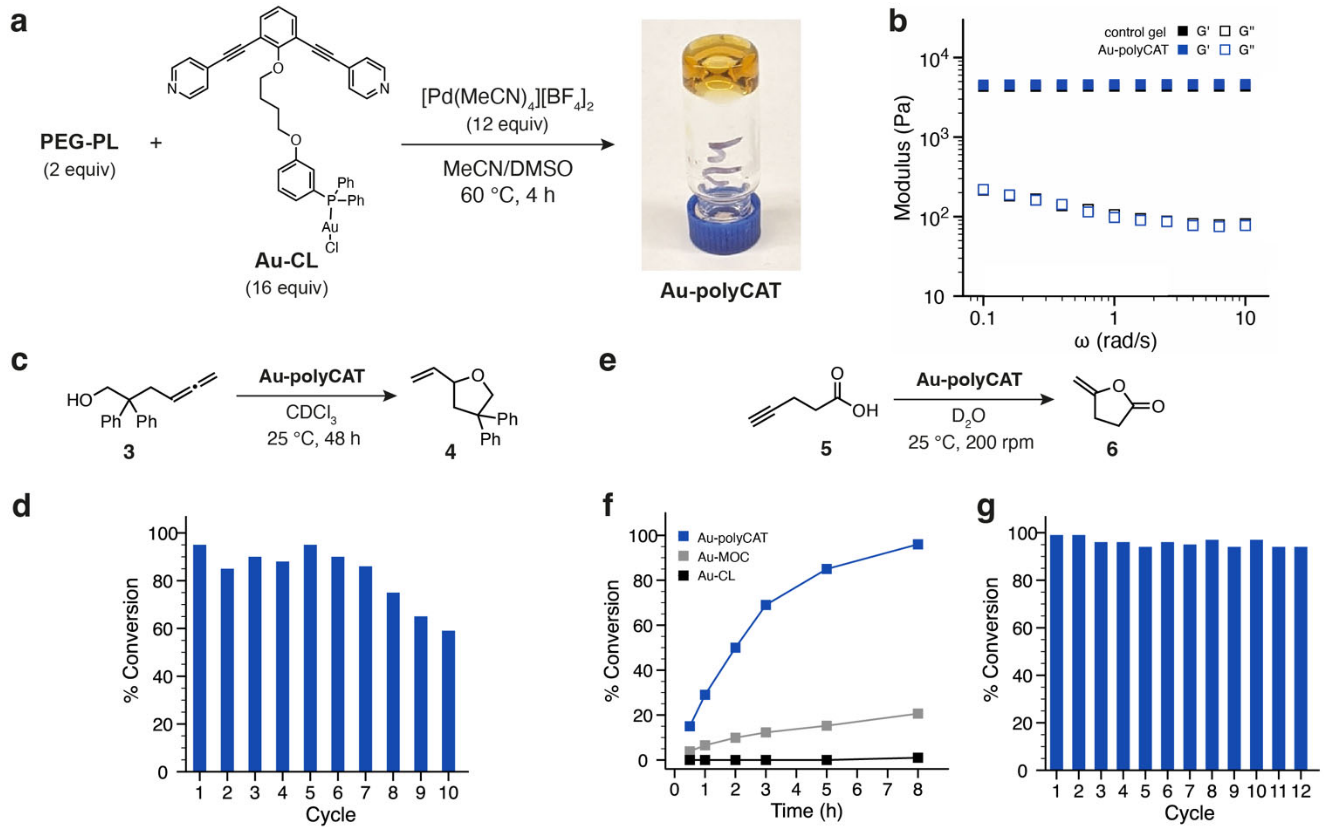

Fig. 3. Use of a Au(I) triphenylphosphine catalyst in the polyCAT system. **a**, Reaction scheme showing **Au-CL** forming **Au-polyCAT** using a similar method as **TEMPO-polyCAT**. **b**, A frequency sweep showing that the **Au-polyCAT** (blue) and a non-CL containing polyMOC (black) have similar material properties. **c**, The cyclization of alleneol (**3**) to its corresponding furan (**4**) using **Au-polyCAT**. **d**, The reaction can be repeated several times using a single **Au-polyCAT** gel in $CDCl_3$ (n=1). **e**, The cyclization of 4-pentynoic acid (**5**) to lactone (**6**) can occur in a solvent (D_2O) in which the catalyst alone (Au-CL) is insoluble. **f**, **Au-polyCAT** greatly outperforms **Au-CL** and **Au-MOC** for the cyclization of **5** to **6** in D_2O (n=1). **g**, The cyclization of **5** using **Au-polyCAT** in D_2O was run for 12 h and repeated 12 times, while maintaining a conversion >94% (n=1). Conversions are calculated from the integrations of the ^{1}H NMR spectrum of the catalytic solution, using an internal standard.

Au-PolyCATs for Au(I)-catalyzed cyclization reactions. Reek and coworkers have reported fascinating homogeneous bis-pyridyl-based Au(I) phosphine complexes (**Au-CL**, Fig. 3a) that are poor catalysts themselves but, due to local concentration effects, function as highly active catalysts when assembled into MOCs through Pd(II) coordination.[58–60] Successful translation of these systems to polyCATs would not only demonstrate modularity of the polyCAT concept but would also provide further evidence for the presence of assembled catalytic MOC junctions within polyCAT networks. Thus, a new polyCAT—**Au-polyCAT**—was prepared following the same procedure used for **TEMPO-polyCAT** but by simply exchanging **TEMPO-CL** for **Au-CL** (here a modified C:P ratio of 2:1 instead of 5:1 was used due to the solubility of **Au-CL**).[58] The SAXS curve for **Au-polyCAT** was very similar to that of **TEMPO-polyCAT** (Figure S4), showing equivalent MOC diameters but a small decrease in the inter-MOC spacing of **Au-polyCAT** as expected from the modified C:P ratio, which gives a greater network branch functionality.

Shear rheology suggested a nearly identical frequency response compared to an analogous control gel prepared from methoxy-functionalized SL with the same C:P ratio (Fig. 3b). These results are remarkable, showing that by simply choosing the CL of interest, **TEMPO-CL** or **Au-CL**, it is possible to generate robust polyCATs from the same PL and Pd(II) salt through simple mixing, offering modularity to heterogeneous catalyst design that would be difficult to predict with traditional (co)polymer systems.

The catalytic activity of **Au-polyCAT** was examined in the context of the intramolecular ring closing of alleneol **3** to form furan **4** (Fig. 3c). A solution of **3** in $CDCl_3$ (0.05 M) containing tetrakis(trimethylsilyl)silane as an internal standard was added to a 2 mL reaction solution containing a 400 mg **Au-polyCAT** gel (0.016 mmol **Au-CL**, 20 mol% relative to alleneol **3**). After 48 h, ~90% conversion of **3** to **4** was observed by ^{1}H NMR spectroscopy, with an initial TOF of 0.1 h^{-1} (Fig. 3d). Moreover, the **Au-polyCAT** maintained >90% of this activity for 7 cycles of the same reaction, achieving 60% conversion after 10 cycles and a TON of 41. As expected based on the work of Reek and colleagues,[58] the reaction proceeded at nearly the same rate as that catalyzed by a homogeneous **Au-MOC**, but reached only 20% conversion when **Au-CL** was used as the catalyst (Fig. S5), supporting the presence of well-assembled MOC junctions within **Au-polyCAT**.[58]

A key potential advantage of the polyCAT system is that through decoupling of the catalyst environment from the polymer support, it could enable catalytic transformations in solvents or conditions where the catalysts are not otherwise compatible. For example, **Au-CL** and **Au-MOC** are not soluble in water; however, due to the polar nature of **PEG-PL**, **Au-polyCAT** swells extensively (swelling ratio of 4.4 in D_2O). As a result, **Au-polyCAT** outperformed **Au-CL** and **Au-MOC** in the cyclization of 4-pentynoic acid (**5**) to **6** in D_2O (Fig. 3e), achieving 96% conversion in 8 h (TOF = 1.2 h^{-1}) compared to 1% for **Au-CL** and 21% for **Au-MOC** (Fig. 3f). While water-soluble gold(I) *N*-heterocyclic carbene[61–63] and triphenylphosphine complexes[64] have been reported for analogous cyclization reactions, catalyst recovery is challenging and has not been demonstrated for these homogeneous systems. By contrast, **Au-polyCAT** could be cycled at least 12 times, with >94% conversion after each 12 h run, achieving a TON of 115 (Fig. 3g). As the recycling runs were 4 h longer than those used to monitor the reaction conversion versus time (12 h vs 8 h), we can state that after 12 × 12 h runs, **Au-polyCAT** maintains >80% of its activity. I.e., on average <2% of the catalyst activity could have been lost per cycle.

An increase in swelling and a 3-fold decrease in G' was observed after these 12 cycles, suggesting some mechanical wearing of the material (Fig. S6). To rule out catalyst leeching from the network due to gel degradation over these 12 cycles, substrate **4** was added to the supernatant of an **Au-polyCAT**-catalyzed reaction; after 8 h, <5% of **4** had cyclized to the lactone product, indicating that the catalytic activity of gel degradation products is negligible. Altogether, these results highlight the potential to use polyCATs under conditions that are not compatible with homogeneous catalyst analogues (e.g., aqueous conditions wherein the catalysts are not soluble) and for facile catalyst recycling.

In order to further demonstrate the modularity of this system using different polymer supports, two new polyCATs were prepared from **Au-CL** by exchanging **PEG-PL** with bis-pyridyl-functionalized linear polystyrene (**PS-PL**, M_n = 31,000, $Đ$ = 1.08) and star poly(*tert*-butyl acrylate) (**PBA-PL**, M_n = 22,000, $Đ$ = 1.09) ligands (Fig. S7, see Supporting Information "Materials and Methods" for full details). The conversion of **5** to **6** in toluene-d_8 solvent was >88% after 8 h for all three of these polyCATs, showing that the same catalyst (**Au-CL**) can be modularly swapped with different polymers even of different architecture (linear versus star) to produce active polyCATs (Fig. S8).

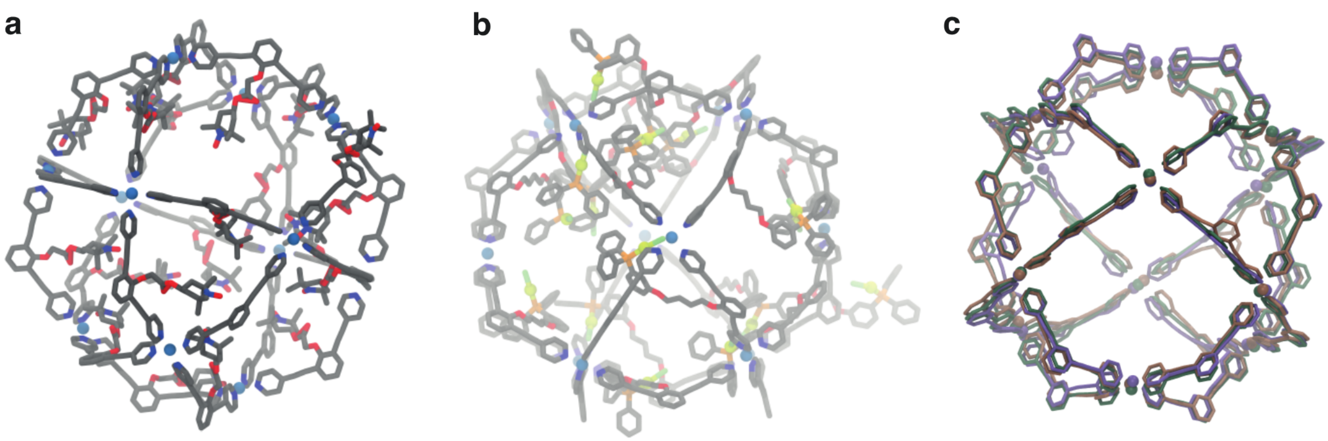

Fig. 4. Calculations of the metal-organic cage (MOC) polyCAT junction structures, using the semi-empirical GFN2-xTB method. **a**, **TEMPO-MOC** and **b**, **Au-MOC** show that incorporations of the catalyst moieties into the MOC does not significantly distort the cage structure. **c**, An overlay of **TEMPO-MOC** and **Au-MOC** (with catalysts omitted for clarity) with a non-catalyst $Pd_{12}L_{24}$ MOC, illustrating that catalyst incorporation maintains the overall MOC geometry.

Finally, to investigate the local catalyst environment within the MOC junctions of polyCATs in more detail, we performed semi-empirical calculations using the GFN2-xTB method[65,66] on MOC junctions at the same C:P ratios used in catalytic studies but without polymers (see Supporting Information section "Calculations" for details). The structures of **TEMPO-MOC** (Fig. 4a), **Au-MOC** (Fig. 4b) and an unsubstituted $Pd_{12}L_{24}$ MOC (Fig. 4c) were optimized using system sizes of 1508, 1596, and 828 atoms, respectively. Structural analysis of the heavy atoms of the palladium cage revealed that the incorporation of 20 **TEMPO-CL** or 16 **Au-CL** species into the $Pd_{12}L_{24}$ MOC structure does not significantly distort the cage structure, with RMSD values of 0.76 and 0.99 Å, with respect to the GFN2-xTB optimized unsubstituted $Pd_{12}L_{24}$ cage. Additionally, these substitutions are energetically favorable via through-space intramolecular interactions between adjacent catalytic ligands as well as between catalytic ligands and the MOC wall. In both the TEMPO and Au(I) cases, the catalysts are largely localized inside the MOC cavity, though a small number were observed to extend outside of the MOC pores due to the flexible linkers employed. Nevertheless, these calculations suggest that MOCs provide a well-defined local environment for catalysis, supporting our polyCAT design.

Conclusions

Herein, we have demonstrated a strategy that allows for the incorporation of homogeneous catalysts into freestanding gels through decoupling catalyst incorporation and environment (within the pores of MOC junctions) from the physical properties of the support (polymer strands). The resulting polyCAT gels form under mild conditions and display robust mechanical properties. Two different CLs (**TEMPO-CL** and **Au-CL**) and three different PLs (**PEG-PL**, **PS-PL**, **PBA-PL**) were used to demonstrate the versatility and modularity of this approach using mechanistically distinct reactions. Freestanding polyCAT gels provided high reaction conversions in each test case, and they could be easily recycled and reused over subsequent reaction cycles, requiring only simple washing between reactions. Additionally, due to the distinct nature of polyCAT junctions versus strands, polyCATs allow catalyst recycling in solvents where the traditional homogeneous catalyst is insoluble (e.g., H_2O). In the future, the polyCAT strategy may leverage the diversity of MOCs of varied shape and composition available today, along with numerous polymer compositions, to facilitate the creation of catalytic materials for a range of synthetic endeavors, potentially simplifying organic synthesis, enabling novel cascade processes and greener manufacturing strategies, and ultimately achieving multi-functional materials that combine the robust mechanical properties of polymer networks with catalytic functions. Finally, the use of semi-empirical calculations to probe the structures of polyCAT junctions will guide the field in the design of future MOC-based catalysts.

Associated Content

The supporting information associated with this manuscript is available free of charge on the internet at ####. Synthetic procedures; gel fabrication; instrumentation details; calculation methods; NMR spectra; EPR data; SAXS data; swelling experiments; catalysis studies.

Corresponding Authors

nathan.oldenhuis@unh.edu

jaj2109@mit.edu

Acknowledgements

CMB acknowledges the Natural Sciences and Engineering Research of Canada (NSERC) for a Postdoctoral Fellowship. DJL acknowledges the National Science Foundation Graduate Research Fellowship Grant No. 1745302 for funding, JRL acknowledges grant 1F32GM126913 for funding, NJO acknowledges grant 1F32GM123710 for funding. This work was supported by the NSF Center for the Chemistry of Molecularly Optimized Networks (MONET), CHE-2116298.

Author Contributions

CMB and DJL contributed equally.

Data Availability

All data for this study are present are available within the Article and its Supplementary Information.

References

(1) Anastas, P. T.; Bartlett, L. B.; Kirchhoff, M. M.; Williamson, T. C. The Role of Catalysis in the Design, Development, and Implementation of Green Chemistry. *Catal. Today* **2000**, *55* (1–2), 11–22. https://doi.org/10.1016/S0920-5861(99)00222-9.

(2) Ludwig, J. R.; Schindler, C. S. Catalyst: Sustainable Catalysis. *Chem* **2017**, *2* (3), 313–316. https://doi.org/10.1016/j.chempr.2017.02.014.

(3) Bystrzanowska, M.; Petkov, P.; Tobiszewski, M. Ranking of Heterogeneous Catalysts Metals by Their Greenness. *ACS Sustain. Chem. Eng.* **2019**, *7* (22), 18434–18443. https://doi.org/10.1021/acssuschemeng.9b04230.

(4) Dumesic, J. A.; Huber, G. W.; Boudart, M. Principles of Heterogeneous Catalysis. In *Handbook of Heterogeneous Catalysis*; Wiley, 2008; pp 1–15.

(5) Corma, A. Heterogeneous Catalysis: Understanding for Designing, and Designing for

Applications. *Angew. Chem. Int. Ed.* **2016**, *55* (21), 6112–6113. https://doi.org/10.1002/anie.201601231.

(6) Pelletier, J. D. A.; Basset, J. M. Catalysis by Design: Well-Defined Single-Site Heterogeneous Catalysts. *Acc. Chem. Res.* **2016**, *49* (4), 664–677. https://doi.org/10.1021/acs.accounts.5b00518.

(7) Vogt, C.; Weckhuysen, B. M. The Concept of the Active Site in Heterogeneous Catalysis. *Nat. Chem. Rev.* **2022**, https://doi.org/10.1038/s41570-021-00340-y. https://doi.org/10.1038/s41570-021-00340-y.

(8) Shende, V. S.; Saptal, V. B.; Bhanage, B. M. Recent Advances Utilized in the Recycling of Homogeneous Catalysis. *Chem. Rec.* **2019**, *19* (9), 2022–2043. https://doi.org/10.1002/tcr.201800205.

(9) Behr, A.; Vorholt, A. J. Introduction. In *Homogeneous Catalysis with Renewables*; Cole-Hamilton, D. J., Van Leeuwen, P. W. N. M., Eds.; Springer, 2017. pp 1–19.

(10) Hübner, S.; De Vries, J. G.; Farina, V. Why Does Industry Not Use Immobilized Transition Metal Complexes as Catalysts? *Adv. Synth. Catal.* **2016**, *358* (1), 3–25. https://doi.org/10.1002/adsc.201500846.

(11) Dioos, B. M. L.; Vankelecom, I. F. J.; Jacobs, P. A. Aspects of Immobilisation of Catalysts on Polymeric Supports. *Adv. Synth. Catal.* **2006**, *348* (12–13), 1413–1446. https://doi.org/10.1002/adsc.200606202.

(12) Benaglia, M.; Puglisi, A.; Cozzi, F. Polymer-Supported Organic Catalysts. *Chem. Rev.* **2003**, *103* (9), 3401–3429. https://doi.org/10.1021/cr010440o.

(13) Ye, R.; Zhukhovitskiy, A. V.; Deraedt, C. V.; Toste, F. D.; Somorjai, G. A. Supported Dendrimer-Encapsulated Metal Clusters: Toward Heterogenizing Homogeneous Catalysts. *Acc. Chem. Res.* **2017**, *50* (8), 1894–1901. https://doi.org/10.1021/acs.accounts.7b00232.

(14) Corma, A.; Garcia, H. Crossing the Borders between Homogeneous and Heterogeneous Catalysis: Developing Recoverable and Reusable Catalytic Systems. *Top. Catal.* **2008**, *48* (1–4), 8–31. https://doi.org/10.1007/s11244-008-9056-5.

(15) Qu, P.; Cleveland, J. W.; Ahmed, E.; Liu, F.; Dubrawski, S.; Jones, C. W.; Weck, M. Compartmentalisation of Molecular Catalysts for Nonorthogonal Tandem Catalysis. *Chem. Soc. Rev.* **2022**, *51*, 57–70. https://doi.org/10.1039/d1cs00530h.

(16) Ikegami, S.; Hamamoto, H. Novel Recycling System for Organic Synthesis via Designer

Polymer-Gel Catalysts. *Chem. Rev.* **2009**, *109* (2), 583–593. https://doi.org/10.1021/cr800481x.

(17) Altava, B.; Burguete, M. I.; García-Verdugo, E.; Luis, S. V. Chiral Catalysts Immobilized on Achiral Polymers: Effect of the Polymer Support on the Performance of the Catalyst. *Chem. Soc. Rev.* **2018**, *47* (8), 2722–2771. https://doi.org/10.1039/c7cs00734e.

(18) Itsuno, S.; Haraguchi, N. Catalysts Immobilized onto Polymers. In *Catalyst Immobilization: Methods and Applications*; Wiley, 2020; pp 23–75. https://doi.org/10.1002/9783527817290.ch2.

(19) Wang, Z.; Liu, H.; Cui, H.; Zhang, M.; Zhang, Z. A Cross-Linked and Swelling Polymer as an Effective Solid Acid Catalyst. *Ind. Eng. Chem. Res.* **2015**, *54* (29), 7219–7225. https://doi.org/10.1021/acs.iecr.5b01408.

(20) Yamada, Y. M. A.; Maeda, Y.; Uozumi, Y. Novel 3D Coordination Palladium-Network Complex: A Recyclable Catalyst for Suzuki-Miyaura Reaction. *Org. Lett.* **2006**, *8* (19), 4259–4262. https://doi.org/10.1021/ol0615026.

(21) Rodríguez-Llansola, F.; Miravet, J. F.; Escuder, B. A Supramolecular Hydrogel as a Reusable Heterogeneous Catalyst for the Direct Aldol Reaction. *Chem. Commun.* **2009**, No. 47, 7303–7305. https://doi.org/10.1039/b916250j.

(22) Rodon Fores, J.; Criado-Gonzalez, M.; Chaumont, A.; Carvalho, A.; Blanck, C.; Schmutz, M.; Serra, C. A.; Boulmedais, F.; Schaaf, P.; Jierry, L. Supported Catalytically Active Supramolecular Hydrogels for Continuous Flow Chemistry. *Angew. Chem. Int. Ed.* **2019**, *58* (52), 18817–18822. https://doi.org/10.1002/anie.201909424.

(23) Wang, G.; Wang, D.; Bietsch, J.; Chen, A.; Sharma, P. Synthesis of Dendritic Glycoclusters and Their Applications for Supramolecular Gelation and Catalysis. *J. Org. Chem.* **2020**, *85* (24), 16136–16156. https://doi.org/10.1021/acs.joc.0c01978.

(24) Zhang, W.; Dynes, J. J.; Hu, Y.; Jiang, P.; Ma, S. Porous Metal-Metalloporphyrin Gel as Catalytic Binding Pocket for Highly Efficient Synergistic Catalysis. *Nat. Commun.* **2019**, *10* (1), 1–8. https://doi.org/10.1038/s41467-019-09881-9.

(25) Liao, P.; Cai, G.; Shi, J.; Zhang, J. Post-Modified Porphyrin Imine Gels with Improved Chemical Stability and Efficient Heterogeneous Activity in CO2 Transformation. *New J. Chem.* **2019**, *43* (25), 10017–10024. https://doi.org/10.1039/c9nj00570f.

(26) Zhang, B.; Reek, J. N. H. Supramolecular Strategies for the Recycling of Homogeneous Catalysts. *Chem. Asian J.* **2021**, *16* (23), 3851–3863. https://doi.org/10.1002/asia.202100968.

(27) Lee, J.; Farha, O. K.; Roberts, J.; Scheidt, K. A.; Nguyen, S. T.; Hupp, J. T. Metal-Organic Framework Materials as Catalysts. *Chem. Soc. Rev.* **2009**, *38* (5), 1450–1459. https://doi.org/10.1039/b807080f.

(28) Zhu, L.; Liu, X. Q.; Jiang, H. L.; Sun, L. B. Metal-Organic Frameworks for Heterogeneous Basic Catalysis. *Chem. Rev.* **2017**, *117* (12), 8129–8176. https://doi.org/10.1021/acs.chemrev.7b00091.

(29) Wu, C. De; Zhao, M. Incorporation of Molecular Catalysts in Metal–Organic Frameworks for Highly Efficient Heterogeneous Catalysis. *Adv. Mater.* **2017**, *29* (14). https://doi.org/10.1002/adma.201605446.

(30) Ma, Q.; Zhang, T.; Wang, B. Shaping of Metal-Organic Frameworks, a Critical Step toward Industrial Applications. *Matter* **2022**, *5* (4), 1070–1091. https://doi.org/10.1016/j.matt.2022.02.014.

(31) Kumar, S.; Mohan, B.; Tao, Z.; You, H.; Ren, P. Incorporation of Homogeneous Organometallic Catalysts into Metal-Organic Frameworks for Advanced Heterogenization: A Review. *Catal. Sci. Technol.* **2021**, *11* (17), 5734–5771. https://doi.org/10.1039/d1cy00663k.

(32) Zhuang, J. L.; Liu, X. Y.; Zhang, Y.; Wang, C.; Mao, H. L.; Guo, J.; Du, X.; Zhu, S. Bin; Ren, B.; Terfort, A. Zr-Metal-Organic Frameworks Featuring TEMPO Radicals: Synergistic Effect between TEMPO and Hydrophilic Zr-Node Defects Boosting Aerobic Oxidation of Alcohols. *ACS Appl. Mater. Interfaces* **2019**, *11* (3), 3034–3043. https://doi.org/10.1021/acsami.8b18370.

(33) Zhang, Z. M.; Zhang, T.; Wang, C.; Lin, Z.; Long, L. S.; Lin, W. Photosensitizing Metal-Organic Framework Enabling Visible-Light-Driven Proton Reduction by a Wells-Dawson-Type Polyoxometalate. *J. Am. Chem. Soc.* **2015**, *137* (9), 3197–3200. https://doi.org/10.1021/jacs.5b00075.

(34) Gascon, J.; Corma, A.; Kapteijn, F.; Llabrés I Xamena, F. X. Metal Organic Framework Catalysis: Quo Vadis? *ACS Catal.* **2014**, *4* (2), 361–378. https://doi.org/10.1021/cs400959k.

(35) Johnson, B. A.; Ott, S. Diagnosing Surface: Versus Bulk Reactivity for Molecular Catalysis within Metal-Organic Frameworks Using a Quantitative Kinetic Model. *Chem. Sci.* **2020**, *11* (28), 7468–7478. https://doi.org/10.1039/d0sc02601h.

(36) Gibbons, B.; Bartlett, E. C.; Cai, M.; Yang, X.; Johnson, E. M.; Morris, A. J. Defect Level and Particle Size Effects on the Hydrolysis of a Chemical Warfare Agent Simulant by UiO-66. *Inorg. Chem.* **2021**, *60* (21), 16378–16387. https://doi.org/10.1021/acs.inorgchem.1c02224.

(37) Kawamoto, K.; Zhong, M.; Wang, R.; Olsen, B. D.; Johnson, J. A. Loops versus Branch Functionality in Model Click Hydrogels. *Macromolecules* **2015**, *48* (24), 8980–8988. https://doi.org/10.1021/acs.macromol.5b02243.

(38) Gu, Y.; Zhao, J.; Johnson, J. A. Polymer Networks: From Plastics and Gels to Porous Frameworks. *Angew. Chem. Int. Ed.* **2020**, *59* (13), 5022–5049. https://doi.org/10.1002/anie.201902900.

(39) Li, R. J.; Pezzato, C.; Berton, C.; Severin, K. Light-Induced Assembly and Disassembly of Polymers with PdnL2n-Type Network Junctions. *Chem. Sci.* **2021**, *12* (13), 4981–4984. https://doi.org/10.1039/d1sc00127b.

(40) Gu, Y.; Zhao, J.; Johnson, J. A. A (Macro)Molecular-Level Understanding of Polymer Network Topology. *Trends Chem.* **2019**, *1* (3), 318–334. https://doi.org/10.1016/j.trechm.2019.02.017.

(41) Foster, J. A.; Parker, R. M.; Belenguer, A. M.; Kishi, N.; Sutton, S.; Abell, C.; Nitschke, J. R. Differentially Addressable Cavities within Metal-Organic Cage-Cross-Linked Polymeric Hydrogels. *J. Am. Chem. Soc.* **2015**, *137* (30), 9722–9729. https://doi.org/10.1021/jacs.5b05507.

(42) Zhukhovitskiy, A. V.; Zhong, M.; Keeler, E. G.; Michaelis, V. K.; Sun, J. E. P.; Hore, M. J. A.; Pochan, D. J.; Griffin, R. G.; Willard, A. P.; Johnson, J. A. Highly Branched and Loop-Rich Gels via Formation of Metal-Organic Cages Linked by Polymers. *Nat. Chem.* **2016**, *8* (1), 33–41. https://doi.org/10.1038/nchem.2390.

(43) Wang, Y.; Zhong, M.; Park, J. V.; Zhukhovitskiy, A. V.; Shi, W.; Johnson, J. A. Block Co-PolyMOCs by Stepwise Self-Assembly. *J. Am. Chem. Soc.* **2016**, *138* (33), 10708–10715. https://doi.org/10.1021/jacs.6b06712.

(44) Zhukhovitskiy, A. V.; Zhao, J.; Zhong, M.; Keeler, E. G.; Alt, E. A.; Teichen, P.; Griffin, R. G.; Hore, M. J. A.; Willard, A. P.; Johnson, J. A. Polymer Structure Dependent Hierarchy in PolyMOC Gels. *Macromolecules* **2016**, *49* (18), 6896–6902. https://doi.org/10.1021/acs.macromol.6b01607.

(45) Wang, Y.; Gu, Y.; Keeler, E. G.; Park, J. V.; Griffin, R. G.; Johnson, J. A. Star PolyMOCs with Diverse Structures, Dynamics, and Functions by Three-Component Assembly. *Angew. Chem. Int. Ed.* **2017**, *56* (1), 188–192. https://doi.org/10.1002/anie.201609261.

(46) Gu, Y.; Alt, E. A.; Wang, H.; Li, X.; Willard, A. P.; Johnson, J. A. Photoswitching Topology in Polymer Networks with Metal–Organic Cages as Crosslinks. *Nature* **2018**, *560* (7716), 65–69.

https://doi.org/10.1038/s41586-018-0339-0.

(47) Oldenhuis, N. J.; Qin, K. P.; Wang, S.; Ye, H. Z.; Alt, E. A.; Willard, A. P.; Van Voorhis, T.; Craig, S. L.; Johnson, J. A. Photoswitchable Sol–Gel Transitions and Catalysis Mediated by Polymer Networks with Coumarin-Decorated Cu24L24 Metal–Organic Cages as Junctions. *Angew. Chem. Int. Ed.* **2020**, *59* (7), 2784–2792. https://doi.org/10.1002/anie.201913297.

(48) Dunning, S. G.; Nandra, G.; Conn, A. D.; Chai, W.; Sikma, R. E.; Lee, J. S.; Kunal, P.; Reynolds, J. E.; Chang, J. S.; Steiner, A.; et al. A Metal–Organic Framework with Cooperative Phosphines That Permit Post-Synthetic Installation of Open Metal Sites. *Angew. Chem. Int. Ed.* **2018**, *57* (30), 9295–9299. https://doi.org/10.1002/anie.201802402.

(49) Zwoliński, K. M.; Chmielewski, M. J. TEMPO-Appended Metal-Organic Frameworks as Highly Active, Selective, and Reusable Catalysts for Mild Aerobic Oxidation of Alcohols. *ACS Appl. Mater. Interfaces* **2017**, *9* (39), 33956–33967. https://doi.org/10.1021/acsami.7b09914.

(50) Li, Z.; Liu, Y.; Kang, X.; Cui, Y. Chiral Metal-Organic Framework Decorated with TEMPO Radicals for Sequential Oxidation/Asymmetric Cyanation Catalysis. *Inorg. Chem.* **2018**, *57* (16), 9786–9789. https://doi.org/10.1021/acs.inorgchem.8b01630.

(51) de Nooy, A. E. J.; Besemer, A. C.; van Bekkum, H. On the Use of Stable Organic Nitroxyl Radicals for the Oxidation of Primary and Secondary Alcohols. *Synthesis (Stuttg).* **1996**, *10*, 1153–1176.

(52) Ueda, Y.; Ito, H.; Fujita, D.; Fujita, M. Permeable Self-Assembled Molecular Containers for Catalyst Isolation Enabling Two-Step Cascade Reactions. *J. Am. Chem. Soc.* **2017**, *139* (17), 6090–6093. https://doi.org/10.1021/jacs.7b02745.

(53) Zhu, F.; Chen, L.; Chen, S.; Qin, Y.; Zhu, F.; Chen, L.; Chen, S.; Wu, G.; Jiang, W.; Shen, J. Article Confinement Self-Assembly of Metal-Organic Cages within Mesoporous Carbon for One-Pot Sequential Reactions Confinement Self-Assembly of Metal-Organic Cages within Mesoporous Carbon for One-Pot Sequential Reactions. *Chem* **2020**, *6* (9), 2395–2406. https://doi.org/10.1016/j.chempr.2020.06.038.

(54) Tominaga, M.; Suzuki, K.; Murase, T.; Fujita, M. 24-Fold Endohedral Functionalization of a Self-Assembled M 12L24 Coordination Nanoball. *J. Am. Chem. Soc.* **2005**, *127* (34), 11950–11951. https://doi.org/10.1021/ja054069o.

(55) Xia, Y.; Li, Y.; Burts, A. O.; Ottaviani, M. F.; Tirrell, D. A.; Johnson, J. A.; Turro, N. J.; Grubbs,

R. H. EPR Study of Spin Labeled Brush Polymers in Organic Solvents. *J. Am. Chem. Soc.* **2011**, *133* (49), 19953–19959. https://doi.org/10.1021/ja2085349.

(56) Kurzbach, D.; Kattnig, D. R.; Zhang, B.; Schlüter, A. D.; Hinderberger, D. Assessing the Solution Shape and Size of Charged Dendronized Polymers Using Double Electron-Electron Resonance. *J. Phys. Chem. Lett.* **2011**, *2* (13), 1583–1587. https://doi.org/10.1021/jz200653k.

(57) Bosman, A. W.; Janssen, R. A. J.; Meijer, E. W. Five Generations of Nitroxyl-Functionalized Dendrimers. *Macromolecules* **1997**, *30* (12), 3606–3611.

(58) Gramage-Doria, R.; Hessels, J.; Leenders, S. H. A. M.; Tröppner, O.; Dürr, M.; Ivanović-Burmazović, I.; Reek, J. N. H. Gold(I) Catalysis at Extreme Concentrations inside Self-Assembled Nanospheres. *Angew. Chem. Int. Ed.* **2014**, *53* (49), 13380–13384. https://doi.org/10.1002/anie.201406415.

(59) Leenders, S. H. A. M.; Dürr, M.; Ivanovic-Burmazovic, I.; Reek, J. N. H. Gold Functionalized Platinum M12L24-Nanospheres and Their Application in Cyclization Reactions. *Adv. Synth. Catal.* **2016**, *358* (9), 1509–1518. https://doi.org/10.1002/adsc.201600071.

(60) Wang, Q. Q.; Gonell, S.; Leenders, S. H. A. M.; Dürr, M.; Ivanovic-Burmazovic, I.; Reek, J. N. H. Self-Assembled Nanospheres with Multiple Endohedral Binding Sites Pre-Organize Catalysts and Substrates for Highly Efficient Reactions. *Nat. Chem.* **2016**, *8* (3), 225–230. https://doi.org/10.1038/nchem.2425.

(61) Tomás-Mendivil, E.; Toullec, P. Y.; Borge, J.; Conejero, S.; Michelet, V.; Cadierno, V. Water-Soluble Gold(I) and Gold(III) Complexes with Sulfonated N-Heterocyclic Carbene Ligands: Synthesis, Characterization, and Application in the Catalytic Cycloisomerization of γ-Alkynoic Acids into Enol-Lactones. *ACS Catal.* **2013**, *3* (12), 3086–3098. https://doi.org/10.1021/cs4009144.

(62) Belger, K.; Krause, N. Smaller, Faster, Better: Modular Synthesis of Unsymmetrical Ammonium Salt-Tagged NHC-Gold(i) Complexes and Their Application as Recyclable Catalysts in Water. *Org. Biomol. Chem.* **2015**, *13* (31), 8556–8560. https://doi.org/10.1039/c5ob01286d.

(63) Lin, B.; Zhang, X.; Zhou, C. Y.; Che, C. M. A PEGylated N-Heterocyclic Carbene-Gold(i) Complex: An Efficient Catalyst for Cyclization Reaction in Water. *Org. Chem. Front.* **2021**, *8* (6), 1216–1222. https://doi.org/10.1039/d0qo01266a.

(64) Elie, B. T.; Levine, C.; Iban, U. B.; Armando, V. R.; Aguilera, R. J.; Ovalle, R.; Contel, M.

Water-Soluble (Phosphane)Gold(I) Complexes - Applications as Recyclable Catalysts in a Three-Component Coupling Reaction and as Antimicrobial and Anticancer Agents. *Eur. J. Inorg. Chem.* **2009**, No. 23, 3421–3430. https://doi.org/10.1002/ejic.200900279.

(65) Grimme, S.; Bannwarth, C.; Shushkov, P. A Robust and Accurate Tight-Binding Quantum Chemical Method for Structures, Vibrational Frequencies, and Noncovalent Interactions of Large Molecular Systems Parametrized for All Spd-Block Elements (Z = 1-86). *J. Chem. Theory Comput.* **2017**, *13* (5), 1989–2009. https://doi.org/10.1021/acs.jctc.7b00118.

(66) Bannwarth, C.; Ehlert, S.; Grimme, S. GFN2-XTB - An Accurate and Broadly Parametrized Self-Consistent Tight-Binding Quantum Chemical Method with Multipole Electrostatics and Density-Dependent Dispersion Contributions. *J. Chem. Theory Comput.* **2019**, *15* (3), 1652–1671. https://doi.org/10.1021/acs.jctc.8b01176.

For Table of Contents Only